

Driving with Prior Maps: Unified Vector Prior Encoding for Autonomous Vehicle Mapping

Shuang Zeng^{1,2*†}, Xinyuan Chang^{1†}, Xinran Liu¹, Zheng Pan¹, Xing Wei^{2‡}

¹Amap, Alibaba Group ²Xi'an Jiaotong University

zengshuang@stu.xjtu.edu.cn, weixing@mail.xjtu.edu.cn

{changxinyuan.cxy, tom.lxr, panzheng.pan}@alibaba-inc.com

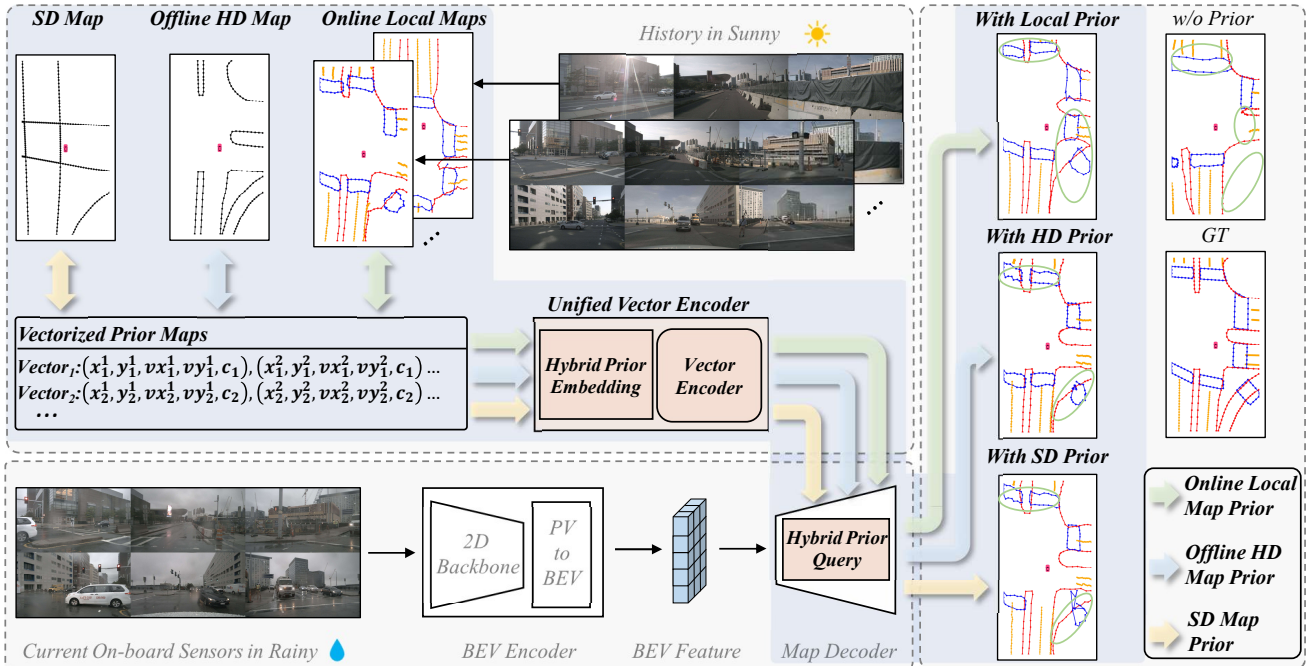


Figure 1. Overview of PriorDrive. Our unified vector encoder (UVE) directly encodes diverse vector prior maps and seamlessly integrates them into existing online mapping frameworks. This integration enhances the final predictions, making them more complete and accurate than those generated without prior information.

Abstract

High-Definition Maps (HD maps) are essential for the precise navigation and decision-making of autonomous vehicles, yet their creation and upkeep present significant cost and timeliness challenges. The online construction of HD maps using on-board sensors has emerged as a promising solution; however, these methods can be impeded by incomplete data due to occlusions and inclement weather. This paper proposes the PriorDrive framework to address these limitations by harnessing the power of prior maps, significantly enhancing the robustness and accuracy of online HD map construction. Our approach integrates a vari-

ety of prior maps, such as OpenStreetMap’s Standard Definition Maps (SD maps), outdated HD maps from vendors, and locally constructed maps from historical vehicle data. To effectively encode this prior information into online mapping models, we introduce a Hybrid Prior Representation (HPQuery) that standardizes the representation of diverse map elements. At the core of PriorDrive is the Unified Vector Encoder (UVE), which employs hybrid prior embedding and a dual encoding mechanism to process vector data. Furthermore, we propose a segment-level and point-level pre-training strategy that enables the UVE to learn the prior distribution of vector data, thereby improving the encoder’s generalizability and performance. Through extensive testing on the nuScenes, Argoverse 2 and OpenLaneV2, we demonstrate that PriorDrive is highly compatible with various online mapping models and substantially im-

* Work done during the internship at Amap, Alibaba Group.

† Equal contribution.

‡ Corresponding author.

proves map prediction capabilities. The integration of prior maps through the PriorDrive framework offers a robust solution to the challenges of single-perception data, paving the way for more reliable autonomous vehicle navigation.

1. Introduction

High-Definition Maps (HD maps) are essential for the accurate navigation and decision-making of autonomous vehicles, providing detailed vectorized representations of road elements such as lane dividers, pedestrian crossings, and road boundaries [6, 8]. Despite their significance, the traditional methods for creating and maintaining HD maps are often costly and labor-intensive. These methods can result in outdated maps that struggle to keep pace with the rapidly changing urban environments. In response, there is increasing interest in online HD map construction [5, 27, 38], where maps are generated in real-time using on-board sensors, such as panoramic RGB cameras and LiDAR point clouds. Although this approach reduces costs, it also introduces new challenges, particularly concerning incomplete and error-prone data caused by environmental occlusions or inclement weather conditions.

In this paper, we introduce **PriorDrive**, a novel framework designed to overcome these challenges by leveraging prior maps. Specifically, PriorDrive incorporates three types of prior maps: Standard Definition Maps (SD maps), existing but outdated HD maps, and online historical prediction maps, as illustrated in Figure 1. SD maps provide essential long-distance centerline skeletons, which are crucial for maintaining road-level connectivity. Existing HD maps (HD map-EX), despite their high accuracy, often fail to reflect current road conditions due to infrequent updates. Nevertheless, these maps offer valuable prior information for HD map construction. Additionally, historical prediction maps, which are often overlooked, can provide insights into current road conditions by reflecting the latest observations from previous perceptions. As vehicles traverse the same locations multiple times under varying conditions, the accumulated information can be used to enhance the quality of the current local map through iterative refinement.

Recent studies [13, 29, 35] have attempted to use prior maps to supplement perception data, but they face several limitations. For instance, NMP [35] relies on a neural prior that cannot take advantage of existing offline maps and can only be updated through model training, leading to poor transferability to new environments. P-MapNet [13] incorporates vector maps into the pipeline by converting them into rasterized representations, which are lossy and redundant, lacking the detail necessary to capture vectorized instance-level information and express the type and direction of map elements effectively. MapEX [29], on the other hand, focuses on existing HD maps but simulates outdated

maps by introducing artificial offsets and erasing map elements, an approach that risks leaking ground truth data and fails to accurately represent the differences between simulated and actual outdated HD maps. These actual outdated maps, due to their low update frequency, struggle to reflect real-time changes in road structures, making them unreliable for current navigation needs.

In addition to constructing accurate online HD maps, the autonomous driving scenario requires understanding the topology in road scenes (*i.e.*, lane connectivity and correspondence with traffic elements), which is called topology reasoning task. Since connected SD maps include crucial information for road topology, we also apply PriorDrive to this task to enhance the performance of topology reasoning.

Given that various maps are typically stored as vectors due to their low redundancy and universal applicability, it’s crucial to develop a robust vector encoding model. However, designing such a model is challenging due to the variable length, sparsity, and discreteness of vector data. To address this and enhance current perception results by integrating diverse vector prior maps into various mapping models, we propose a unified vector encoder (UVE). The UVE can encode a wide range of vector data types, and we introduce pre-training paradigms that allow model to fully learn the prior distribution of vector maps. Our experiments on nuScenes, Argoverse 2 and OpenLane-V2 demonstrate that our PriorDrive is plug-and-play and can be seamlessly applied to various online mapping models and vector tasks, resulting in significant performance improvements.

In summary, our contributions are as follows:

- We introduce a unified vector encoder that effectively captures diverse vector attributes and enables encoding of variable-length vectors into fixed-length features through Hybrid prior embedding and dual encoding mechanism.
- We first proposed a pre-training paradigm for vector data, which can effectively learn the prior distribution of vector data and help reduce noise in historical maps through point-level and segment-level pre-training.
- We propose a hybrid prior representation (HPQuery) to represent all elements and a PriorDrive framework with vector prior maps to addresses the limitations of single-perception. Our comprehensive evaluation demonstrates that PriorDrive is plug-and-play and significantly enhances the performance of online mapping models.

2. Related work

2.1. Online vectorized HD map construction

Online vectorized HD map construction was initially treated as a segmentation task [15, 18]. To construct vectorized HD map, HDMaNet [15] requires complex post-processing of pixel-level rasterized maps. VectorMapNet [25] introduced a coarse-to-fine, two-stage network leveraging key-

point representations. MapTR [19] advanced this concept by modeling point sets in a permutation-equivalent manner using a DETR-like [2] one-stage network. Subsequent studies [3, 9, 12, 36, 39–41] have introduced various insightful approaches for further improvement. However, these methods rely solely on single-source perception data from vehicle-mounted sensors, limiting their effectiveness in challenging scenarios such as occlusion or inclement weather conditions.

The release of OpenLane-V2 [31] dataset has sparked growing interest in topology reasoning within driving scenes. This task focuses on recognizing the topologies among lanes and lanes with traffic elements. TopoNet [17] leverages GNN to update lane representation and lane topology. TopoMLP [34] utilizes PETR [24] for centerline detection and employs simple MLPs to predict the relationships. In this paper, we also apply PriorDrive to topological inference tasks, introducing interconnected SD Map as an additional input to support topology reasoning.

2.2. Online mapping based on prior maps

Recent research has explored the integration of prior maps to enhance the performance of online mapping models. P-MapNet [13] encodes Standard Definition Maps (SD map) as an additional conditional branch and employs a masked autoencoder to capture the prior distribution of HD maps. NMP [35] introduces a global neural map prior that self-updates, thereby improving the performance of local map inference. MapEX [29] categorizes existing maps into three types and refines the query-based map estimation model’s matching algorithm. Despite these advances, many studies overlook the potential of online historical prediction maps as a source of prior information. Our work addresses this gap by leveraging various existing prior maps in their native vector form to enhance current perception data.

2.3. Pretrained methods based on mask modeling

In the fields of NLP and CV, masked pre-training has proven to be an effective strategy for self-supervised representation learning. In NLP, models like BERT [4, 14, 23] use masked language modeling to predict randomly masked tokens within a bidirectional text context. Similarly, methods such as MAE [11, 16, 21] mask random patches of input images and reconstruct them based on the remaining unmasked patches. Diverging from these approaches, which are predominantly tailored for text and image data, we introduce a pre-training paradigm specifically designed for vector data. Our method aims to learn the prior distribution of vector representations, offering a new avenue for pre-training in the context of vectorized data.

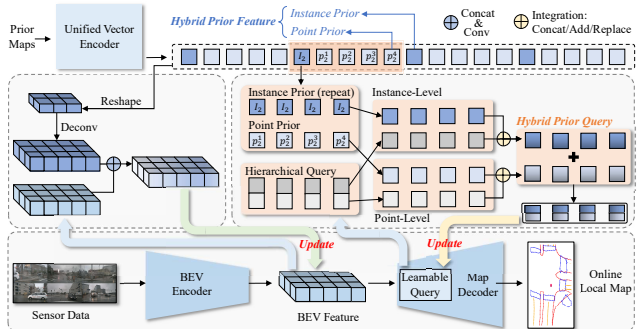


Figure 2. Our Integration Method. For query-based models, we enable interaction between the prior features and queries at both instance-level and point-level, ensuring a more nuanced integration. Hierarchical query comes from MapTRv2 [20]. For the other models, we integrate prior features directly with the BEV features.

3. Proposed method: PriorDrive

3.1. Problem formulation

Formulation of online mapping. The goal of online mapping is to construct a local HD map using on-board sensor observations, such as the surrounding camera images. The online mapping process typically involves two main modules: the Bird’s-Eye View (BEV) encoder and the map decoder. The BEV encoder generally includes a Perspective View (PV) feature extractor and a module for transforming PV features into BEV features. The map decoder usually comprises a Fully Convolutional Network [28] or a query-based module similar to DETR [2], which outputs either rasterized perception results or vectorized map elements.

Let the set of images be denoted as $\{I_1, \dots, I_k\}$, and the BEV encoder be represented as E_{bev} . The extraction of BEV features f_{bev} can then be expressed as:

$$f_{bev} = E_{bev}(\{I_1, \dots, I_k\}). \quad (1)$$

Similarly, let the map decoder module be denoted as D_{map} . The final process of predicting map elements can be expressed as:

$$\mathcal{P} = D_{map}(f_{bev}, opt(Q)), \quad (2)$$

where \mathcal{P} represents the predicted map elements, Q denotes the learnable query, and opt indicates that this learnable query is optional, which is required in query-based models but not in other models.

Extraction of prior map features. Our proposed UVE serves as a unified vector encoder that can directly encode various vector data information, such as the position (x, y) , direction (v_x, v_y) , and type of points (c) . Using $p = [x, y, v_x, v_y, c]$ to represent the point, a vector v typically consists of multiple ordered sets of points, $v =$

$[p_1, p_2, \dots, p_n]$, where n varies. The map prior M_{prior} consists of multiple vectors $M_{prior} = \{v_1, v_2, \dots, v_m\}$, with m being variable. Using E_{uve} to represent the UVE model, the extraction process of the features of the prior map, denoted as f_{prior} , can be represented as:

$$f_{prior} = E_{uve}(M_{prior}). \quad (3)$$

Online mapping based on prior maps. We proposed four methods in total to integrate prior map features into online mapping models. For the methods without a learnable query Q , such as HDMapNet [15], we directly reshape the prior feature f_{prior} and use $Deconv$ upsampling to match the shape of the BEV feature f_{bev} . Then connect it with the BEV feature f_{bev} and aligned by $Conv$, as shown in Figure 2 left.

$$f_{bev}^* = Conv(cat[f_{bev}, Deconv(reshape(f_{prior}))]), \quad (4)$$

here, f_{bev}^* represents BEV feature after incorporating the prior map information, which can be input into the map decoder D_{map} to obtain the predicted results of map elements.

For methods based on learnable query Q , such as the vectorized model MapTR series [20], we propose HPQuery of three operations: addition, replacement, and concatenation, as shown in Figure 2 right. Specifically, Q is typically composed of two parts, $Q = \{q_{ij}\}_{i=0, j=0}^{m, n} = \{q_i^{ins} + q_j^{pt}\}_{i=0, j=0}^{m, n}$, q_i^{ins} and q_i^{pt} representing the learnable queries at the instance-level and point-level respectively. The features f_{prior} of prior maps are also composed of instance-level features and point-level features, $f_{prior} = \{(f_i^{ins}, f_j^{pt})\}_{i=0, j=0}^{m', n'}$. So we interact prior features and queries at the instance level and click, respectively. The HPQuery of addition, replacement, and concatenation operations can be expressed as:

$$q_{ij}^* = q_i^{ins}.add(f_i^{ins}) + q_j^{pt}.add(f_j^{pt}), \quad (5)$$

$$q_{ij}^* = q_i^{ins}.replace(f_i^{ins}) + q_j^{pt}.replace(f_j^{pt}), \quad (6)$$

$$q_{ij}^* = concat[q_i^{ins}, f_i^{ins}] + concat[q_j^{pt}, f_j^{pt}]. \quad (7)$$

We will detail the effectiveness of these feature fusion methods in the experimental section.

3.2. Architecture of UVE

Inspired by BERT [4] on text-related tasks, we propose a unified vector encoder (UVE) by analogizing vector points to words and vector map elements to sentences (see Figure 3). And we provide a pre-training strategy to improve the encoding and noise reduction ability of UVE.

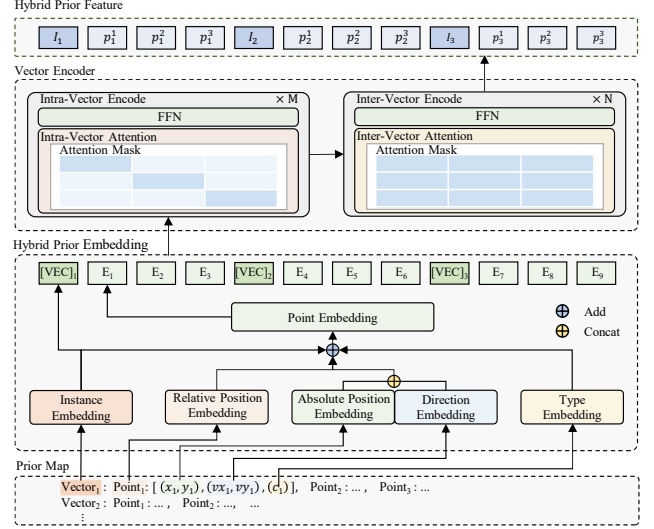


Figure 3. Structure of UVE. Hybrid prior embedding enhances vector representation. Intra-instance and inter-instance attention mechanisms are employed to refine local features and capture global context effectively.

Hybrid prior embedding. As shown in Figure 3, for the given prior map M_{prior} , we first construct the input for UVE, termed as Hybrid Prior Embedding (HPE). We use the method from [30] for obtaining point position embedding and direction embedding for both (x, y) and (v_x, v_y) . We concatenate these two embeddings as the point-level embedding. To obtain the feature representation of the entire vector, we add a special $[VEC]$ token at the beginning of each vector and use the embedding of this token as the instance-level embedding. Additionally, we introduce learnable instance embedding and learnable type embedding to distinguish vector instances. To ensure the order of points, we also introduce 2D learnable position embedding. Finally, these embeddings are aggregated to form the HPE, which then serves as the input embedding for UVE.

Dual encoding mechanism. Due to the limited information content of vector points themselves, learning the concept of vector instances is very challenging for the model, requiring more interactions among the points within the vectors to enhance each point's perceptual abilities towards others in the same vector. As a result, the UVE encoder utilizes M -layer intra-vector attention encoders and N -layer inter-vector attention encoders, using an attention masking mechanism to facilitate feature interactions within and between different vector instances.

3.3. Pre-training UVE: Position modeling

Due to the limited inference ability of online mapping model, there are errors in historical prediction maps. So we

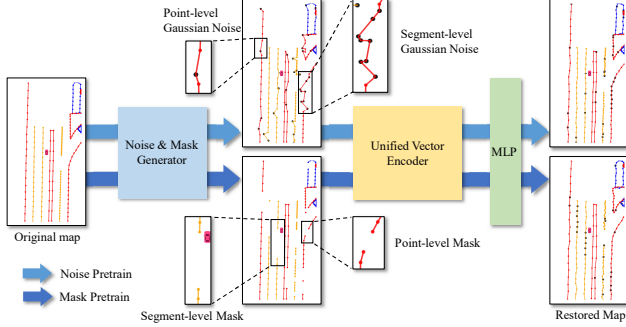


Figure 4. Pre-trained Pipeline. The noise & mask generator creates segment-level and point-level noise or mask, and then reconstructs the entire map via UVE and MLP.

used position modeling to pre-train UVE to improve its encoding and noise reduction capabilities. Specifically, there are two methods: random noise and masking (see Figure 4).

Noise & mask generator. The noise is primarily categorized into segment-level and point-level. In point-level noise, random noise is added to 5% of the vector points across the entire map. For segment-level noise, random noise is added to all vector points within a sub-vector segment, after randomly selecting 10% of the map elements. Using M_{org} to represent the original map elements (with the same data structure as M_{prior}), the process of adding Gaussian noise can be represented by the following formula:

$$M_{org}^* = M_{org}[random_index] + \epsilon, \quad (8)$$

where $\epsilon \sim \mathcal{N}(0, 1)$ is a random noise, which is only added to the horizontal and vertical coordinates of each point.

Similar to adding noise to the points, the selection of points for adding the mask is also divided into point-level and segment-level. After selecting the points to add the mask, the coordinates of these points will be masked as -1 .

$$M_{org}^* = M_{org}[random_index].replace(Mask). \quad (9)$$

Loss function. We feed the vector map to UVE encoding after passing through the noise mask generator, then decode the coordinates of all vector points using MLP, and calculate mean euclidean distance from real coordinates as supervision:

$$\mathcal{L} = RMSE(P, mlp(E_{uve}(M_{org}^*))), \quad (10)$$

where $P = \{(x_i, y_i)\}_{i=0}^k$ represent all the point in M_{org} .

4. Experiments

4.1. Experimental settings

Benchmark. We mainly validate our method on the popular nuScenes [1] and Argoverse 2 [33] following the stan-

dard setting of previous methods [19, 25]. NuScenes contains a total of 1,000 scenes, each with an approximate duration of 20 seconds. The data was collected utilizing a 32-beam LiDAR operating and six cameras offering a 360-degree field of view. Argoverse 2 includes 1000 logs, each offering 15 seconds of 20Hz RGB images captured from 7 cameras, along with a 3D vector map.

Furthermore, to demonstrate that PriorDrive is plug-and-play and widely applicable to other vector tasks, we conducted a topology inference task on OpenLane-V2 [31] dataset. Subset A, developed by Argoverse 2 [33], includes seven views as input, along with an additional SD map.

Evaluation protocol. For the vectorized results, we follow the standard metric used in previous works [15, 19, 25]. The perception range along the direction of vehicle travel are $[-15.0m, 15.0m]$ for the X -axis and $[-30.0m, 30.0m]$ for the Y -axis. And we adopt average precision (AP) evaluated the quality of map construction. We compute the AP_τ under several Chamfer distance $D_{Chamfer}$ thresholds ($\tau \in T, T = \{0.5, 1.0, 1.5\}$), and then calculate the mean across all thresholds as the final AP metric:

$$AP = \frac{1}{|T|} \sum_{\tau \in T} AP_\tau. \quad (11)$$

Furthermore, to evaluate the effectiveness of our method across different evaluation metrics and for the rasterized results, we follow the previous works [13, 15, 35] and employ IoU as the metrics for segmentation results.

For OpenLane-V2's lane centerline perception task, DET_l averages the Fréchet distance to quantify similarity. DET_t uses IoU and averages it across various traffic categories. TOP_l and TOP_t compute the topology matrix similarity between lanes and between lanes and traffic elements, respectively. The overall metric is called OLS:

$$OLS = \frac{1}{4} [DET_l + DET_t + f(TOP_l) + f(TOP_t)], \quad (12)$$

where f is the square root function.

Implementation details. For fair comparisons, experiments were conducted on all baseline models using their original configs and parameters without any changes. All experiments were trained with 6 NVIDIA RTX A6000. For pre-training UVE, we trained the 24-epoch on nuScenes vector data. For historical prediction maps, we run each base model to get their respective online local maps.

4.2. Main results

Results on nuScenes. To evaluate the effectiveness of our method across different model, evaluation metrics, and vector prior maps, we choose HDMaNet and MapTRv2 as

Method	Modality	Backbone	Epoch	Metric	ped.	div.	bou.	mean	$\tau_{0.5m}$
HDMapNet [15]	C	Effi-B0	30	IoU	18.7	40.6	39.5	32.9	-
# SD map Prior (Ours)	C	Effi-B0	30	IoU	22.2	42.0	41.5	35.2	-
# Online Local Map Prior (Ours)	C	Effi-B0	30	IoU	23.1	41.4	42.0	35.5	-
# HD map-EX* Prior (Ours)	C	Effi-B0	30	IoU	21.2	42.3	44.9	36.1	-
MapTR [19]	C	R50	24	AP	41.2	49.5	51.1	47.3	-
# P-MapNet [13]	C	R50	24	AP	43.7	50.9	53.5	49.4	-
StreamMapNet [37]	C	R50	24	AP	60.4	61.9	58.9	60.4	-
# SQD-MapNet [32]	C	R50	24	AP	63.0	65.5	63.3	63.9	-
MGMap [22]	C	R50	24	AP	61.8	65.0	67.5	64.8	-
MapTRv2 [20]	C	R50	24	AP	59.8	62.4	62.4	61.5	38.6
# SD map Prior (Ours)	C	R50	24	AP	61.7	65.5	66.4	64.5	42.7
# Online Local Map Prior (Ours)	C	R50	24	AP	63.6	67.3	66.2	65.7	44.7
# HD map-EX* Prior (Ours)	C	R50	24	AP	61.5	65.6	68.3	65.1	44.3

Table 1. Performance of various online mapping models with different prior maps on nuScenes within a $60m \times 30m$ perception range. ‘‘C’’ denotes camera input. The SD map is sourced from OpenStreetMap [10]. The online local map refers to the historical prediction results. As the nuScenes dataset lacks existing HD maps, we followed the approach of MapEX [29] to create an HD map-EX*, simulating existing HD maps by removing pedestrian crossings and lane dividers, while retaining only the road boundaries.

Method	AP_{ped}	AP_{div}	AP_{bou}	mAP
MGMap [22]	52.8	67.5	68.1	62.8
MapQR [26]	60.1	71.2	66.2	65.9
MapTRv2 [20]	60.7	68.9	64.5	64.7
# SD Prior (Ours)	62.0	70.2	66.3	66.2
# Online Local Prior (Ours)	63.9	71.7	68.6	68.1
# HD map-EX* (Ours)	61.5	69.8	69.4	66.9

Table 2. Comparison on Argoverse 2 where the 3D map elements are predicted directly.

baselines (see Table 1). SD maps, which primarily consists of a centerline skeleton, showed enhancements of 3.0 mAP for MapTRv2 and 2.3 mIoU for HDMapNet, respectively. And for query-based model, our method has a greater improvement because our HPQuery makes better use of prior maps. Online local maps, which offer up-to-date information, led to more significant improvements, with 4.2 mAP and 2.6 mIoU for MapTRv2 and HDMapNet, respectively. These results indicate that more accurate and current local maps contribute to better performance by providing more comprehensive and precise information. Figure 5 illustrates how online local maps effectively restore obscured map elements. More visualization are shown in the supplementary material. Although offline HD maps are highly accurate, their lack of complete prior information resulted in notable improvements of 3.6 mAP and 3.2 mIoU for MapTRv2 and HDMapNet, respectively. Additionally, we evaluated the results using a stricter threshold of 0.5m, achieving improvements of 4.1 mAP, 6.1 mAP, and 5.7 mAP, respec-

Method	DET_l	DET_t	TOP_{ll}	TOP_{lt}	OLS
MapTR [19]	17.7	43.5	5.9	15.1	31.0
TopoNet [17]	28.6	48.6	10.9	23.8	39.8
TopoLogic [7]	29.9	47.2	23.9	25.4	44.1
# SD Prior (Ours)	29.9	47.1	29.6	32.9	47.2
# Online Local Prior (Ours)	31.0	47.8	30.9	32.5	47.9

Table 3. Performance comparison with SOTA methods on OpenLaneV2 subset_A set, where SD Prior comes from the SD map of the openLanev2 itself. Since the map elements here have only centerline and no boundaries, there is no HD map-EX* prior.

tively, underscoring that our method provides more substantial improvements under stricter evaluation conditions. Overall, our method demonstrated consistent performance improvements across all baselines with various prior maps, highlighting its generalizability and potential applicability to other mapping frameworks.

Results on Argoverse 2. In Table 2, we present the results of Argoverse 2, which provides 3D vectorized map elements with additional height information as ground truth. These testings are all trained 6 epochs with ResNet50 as the backbone. Our PriorDrive improves performance by 1.5, 3.4, and 2.2, respectively, using different prior maps, demonstrating the superior generalization ability of PriorDrive in terms of 3D vectorized map construction.

M	N	Dim	IoU			
			ped.	div.	bou.	mean
4	4	64	20.7	41.3	41.1	34.4
6	2	64	20.5	41.1	40.9	34.2
2	6	64	20.7	41.0	41.3	34.3
2	2	128	19.5	41.4	41.2	34.0
2	2	64	20.8	41.7	41.8	34.8
1	1	32	19.8	41.1	40.9	33.9

Table 4. Ablation experiments on UVE structure within HDMaNet and SD map prior.

Method Type	Seg	Pt	Dist Err	AP			
				ped.	div.	bou.	mean
Without Pretrain			-	61.3	63.4	64.4	63.0
Original	-	-	0.09m	61.2	64.1	64.5	63.3
Noise 3m	20%	-	0.46m	61.4	63.0	63.8	62.7
Noise 1m	10%	-	0.15m	61.6	63.8	64.2	63.2
Noise 1m	10%	5%	0.18m	61.6	64.3	64.8	63.6
*Noise 1m	10%	5%	0.20m	62.5	66.3	64.5	64.4
Mask	10%	5%	0.43m	61.8	64.0	64.3	63.4

Table 5. Ablation of the pre-training strategies. Here, we fixed *prior_num=multiple*, *search_range=5m* and *integration=replace*. “Seg” and “Pt” represent segment-level and point-level, respectively. * indicates data augmentation to expand the data volume.

Results on OpenLane-V2. We compared PriorDrive with SOTA methods when using ResNet-50 for training 24 epochs. Table 3 shows the results on subset A of OpenLane-V2. Compared to TopoLogic, our method achieves better topological reasoning accuracy using connected SD priors (29.6 v.s. 23.9 on TOP_{lt} , 32.9 v.s. 25.4 on TOP_{lt}), and the overall score OLS increased by 3.1, indicating that connected SD is more beneficial for lane connectivity and correspondence with traffic elements. Employing online local priors resulted in decent detection accuracy for both detection and topological reasoning, with OLS rising to 47.9. Overall, PriorDrive is a plug-and-play solution that can be widely applied to other vector tasks.

4.3. Ablation study

In this section, we do extensive research on UVE structure, pre-training, number and search range of prior maps, and integration methods. we conduct experiments using online local map priors on MapTRv2 unless otherwise specified.

Structure of UVE. Table 4 presents the results of ablation experiments on the UVE structure using the SD prior map within HDMaNet. We observed that increasing the num-

Fixed Parameters	Prior Num	AP			
		ped.	div.	bou.	mean
-	None	59.8	62.4	62.4	61.5
<i>search_range=5m</i> <i>pretrain=true</i> <i>integration=replace</i>	One	61.1	63.8	63.6	62.8
	Two	61.4	66.2	63.0	63.5
	Multiple	62.5	66.3	64.5	64.4

Table 6. Ablation experiments on the number of online local prior maps on MapTRv2.

Fixed Parameters	Search Range	AP			
		ped.	div.	bou.	mean
-	None	59.8	62.4	62.4	61.5
<i>prior_num=2</i> <i>pretrain=true</i> <i>integration=replace</i>	5 m	62.5	66.3	64.5	64.4
	10 m	61.4	64.6	64.4	63.5
	15 m	61.9	63.2	63.9	63.0

Table 7. Ablation experiments on the search range of online local prior maps on MapTRv2.

ber of layers or expanding the feature dimension of UVE yielded only marginal improvements, averaging around 1.3 mIoU. This limited gain may be attributed to the model’s excess capacity, leading to overfitting. Conversely, a minimal configuration of UVE, with only one layer each of intra-vector and inter-vector attention and a dimension of 32, resulted in a modest improvement of just 1 mIoU. However, when UVE was configured with two layers of intra-vector and inter-vector attention and a feature dimension of 64, the model’s performance reached saturation.

The effect of pre-training. To effectively capture the prior information of vector maps, we pre-trained UVE using different strategies in Table 5. When we fed the original vector map directly to UVE without any noise, UVE converged with a minimal error of 0.09 meters. However, the simple task might have limited the model’s ability to fully learn the prior distribution, resulting in only a 0.3 mAP improvement. We added segment-level Gaussian noise with a 3-meter standard deviation to 20% of the map elements randomly. The UVE’s average Euclidean distance error was 0.46 meters. However, this approach led to a slight decrease in mAP, likely because the UVE had not fully converged. Next, we applied 1-meter segment-level noise to 10% of the map elements randomly, resulting in a reduced error of 0.15 meters for UVE and a 0.2 mAP improvement compared to the model without pre-training. Building on this, we introduced 1-meter point-level noise to 5% of the vector points. Although this increased UVE’s error to 0.18 meters, it yielded a more substantial mAP improvement of 0.6. This

Fixed Parameters	Integrated Method	AP			
		ped.	div.	bou.	mean
-	None	59.8	62.4	62.4	61.5
<i>prior_num=2</i> <i>pretrain=true</i> <i>search_range=5m</i>	Replace	62.5	66.3	64.5	64.4
	Add	63.3	64.1	64.4	63.9
	Concat	63.6	67.3	66.2	65.7

Table 8. Ablation experiments on the integrated methods of online local prior maps on MapTRv2.

demonstrates that pre-training strategies incorporating both segment-level and point-level noise are more effective at learning the prior information of vector maps. We also experimented with masking instead of noise, which increased UVE’s error to 0.43 meters but still resulted in a 0.4 mAP improvement. Although various proposed tasks can effectively pre-train UVE, they are still limited by the amount of pre-training data. Therefore, we employ horizontal and vertical flipping data augmentation to expand the pre-training dataset. The result of the data augmentation is shown as *, effectively improving 1.4 mAP.

Impact of the number of prior maps. We conducted an ablation study to assess the effect of the number of prior maps on model performance (see Table 6). The results indicate that using a single prior map led to a 1.3 mAP improvement, demonstrating its effectiveness in enhancing current perception. Incorporating two prior maps resulted in a more substantial improvement of 2.0 mAP, reflecting the value of richer prior information. Finally, multiple prior maps effectively improved 2.9 mAP, indicating that more prior maps can provide more comprehensive necessary information.

Effect of different search ranges for prior maps. We performed ablation experiments to explore the impact of search ranges for prior maps in Table 7. The results indicate that increasing the search range leads to a slight decrease in improvement. This suggests that while a larger search range allows the prior map to cover a wider area, it also introduces greater positional error. On the other hand, a more precise, narrower search range may not always provide multiple prior maps for most locations, limiting the benefits.

Different methods for integrating prior maps. To evaluate the versatility of our approach, we tested various integration methods in Table 8. Compared to MapTRv2, the HPQuery methods of replacement and addition resulted in mAP improvements of 2.9 and 2.4, respectively, but these methods may impact the performance of the original query. In contrast, the concatenation method achieved a more substantial improvement of 4.2 mAP. This approach effectively

-	MapTRv2	Ours
FPS	10.3	9.9
GPU mem (MB)	2624	2650
Params (MB)	40.3	43.4
mAP	61.5	65.7

Component	Runtime (ms)	Proportion
2D Backbone	47.6	50.2%
PV to BEV	12.9	13.6%
UVE	14.6	15.3%
Map Decoder	19.8	20.9%

Table 9. Detailed comparison of our method with MapTRv2. FPS and detailed runtime of each component are measured on one A6000 GPU with batch size as 1.

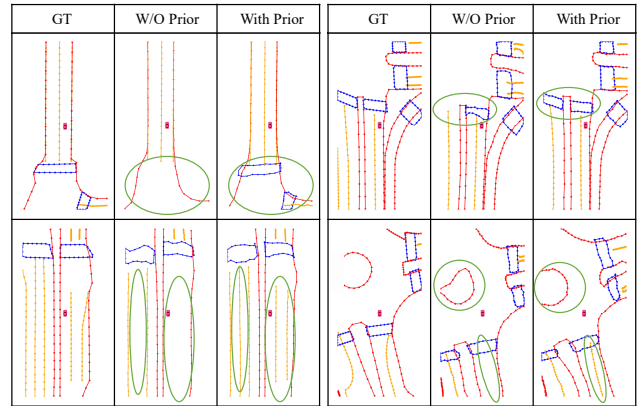


Figure 5. Qualitative results with and w/o online local prior.

preserves the original query’s integrity while also leveraging the instance-level and point-level prior features learned by UVE, making it the most effective integration method.

Inference speed, memory, model size, and detailed runtime. Table 9 compares our method with MapTRv2 in the above aspects. The results show that our method maintains similar FPS, GPU memory usage, and parameter count compared to MapTRv2, while achieving a 4.2 mAP improvement. Additionally, we provide the detailed runtime of each component. Our proposed UVE accounts for only 15.3% of the total pipeline runtime, with the majority of inference time spent on the 2D Backbone (50.2%), highlighting the efficiency and practical value of our approach across various application scenarios.

5. Conclusion

In this paper, we introduced PriorDrive, a novel framework that effectively leverages various types of prior maps to enhance the accuracy and robustness of online HD map con-

struction. Central to PriorDrive is UVE, which can encode diverse vector data efficiently. Through comprehensive experiments, we demonstrated that UVE, combined with proposed pre-training strategies, significantly improves performance of state-of-the-art models in various vector tasks. PriorDrive not only addresses the challenges associated with online HD map construction in complex environments but also offers a scalable solution that continually improves accuracy over time. The iterative use of historical prediction maps as priors leads to progressively refined map outputs, providing latest road information for autonomous driving.

References

- [1] Holger Caesar, Varun Bankiti, Alex H. Lang, Sourabh Vora, Venice Erin Liong, Qiang Xu, Anush Krishnan, Yuxin Pan, Giancarlo Baldan, and Oscar Beijbom. nuscenes: A multi-modal dataset for autonomous driving. In *CVPR*, 2019. 5
- [2] Nicolas Carion, Francisco Massa, Gabriel Synnaeve, Nicolas Usunier, Alexander Kirillov, and Sergey Zagoruyko. End-to-end object detection with transformers. In *ECCV*, 2020. 3
- [3] Jiacheng Chen, Yuefan Wu, Jiaqi Tan, Hang Ma, and Yasutaka Furukawa. Maptracker: Tracking with strided memory fusion for consistent vector hd mapping. In *ECCV*, 2024. 3
- [4] Jacob Devlin, Ming-Wei Chang, Kenton Lee, and Kristina Toutanova. Bert: Pre-training of deep bidirectional transformers for language understanding. In *NAACL*, 2019. 3, 4
- [5] Wenjie Ding, Limeng Qiao, Xi Qiu, and Chi Zhang. Pivotnet: Vectorized pivot learning for end-to-end hd map construction. In *ICCV*, 2023. 2
- [6] Gamal Elghazaly, Raphaël Frank, Scott Harvey, and Stefan Saffko. High-definition maps: Comprehensive survey, challenges, and future perspectives. *IEEE OJ-ITS*, 2023. 2
- [7] Yanping Fu, Wenbin Liao, Xinyuan Liu, Hang xu, Yike Ma, Feng Dai, and Yucheng Zhang. Topologic: An interpretable pipeline for lane topology reasoning on driving scenes, 2024. 6
- [8] Jiyang Gao, Chen Sun, Hang Zhao, Yi Shen, Dragomir Anguelov, Congcong Li, and Cordelia Schmid. Vectornet: Encoding hd maps and agent dynamics from vectorized representation. In *CVPR*, 2020. 2
- [9] Xunjiang Gu, Guanyu Song, Igor Gilitschenski, Marco Pavone, and Boris Ivanovic. Producing and leveraging online map uncertainty in trajectory prediction. In *CVPR*, 2024. 3
- [10] Mordechai (Muki) Haklay and Patrick Weber. Openstreetmap: User-generated street maps. *IEEE Pervasive Computing*, 2008. 6
- [11] Kaiming He, Xinlei Chen, Saining Xie, Yanghao Li, Piotr Dollár, and Ross B. Girshick. Masked autoencoders are scalable vision learners. In *CVPR*, 2021. 3
- [12] Haotian Hu, Fanyi Wang, Yaonong Wang, Laifeng Hu, Jingwei Xu, and Zhiwang Zhang. Admap: Anti-disturbance framework for reconstructing online vectorized hd map. In *ECCV*, 2024. 3
- [13] Zhou Jiang, Zhenxin Zhu, Pengfei Li, Huan-ang Gao, Tianyuan Yuan, Yongliang Shi, Hang Zhao, and Hao Zhao. P-mapnet: Far-seeing map generator enhanced by both sdmap and hdmap priors. *arXiv preprint arXiv:2403.10521*, 2024. 2, 3, 5, 6
- [14] Zhenzhong Lan, Mingda Chen, Sebastian Goodman, Kevin Gimpel, Piyush Sharma, and Radu Soricut. Albert: A lite bert for self-supervised learning of language representations. *arXiv preprint arXiv:1909.11942*, 2019. 3
- [15] Qi Li, Yue Wang, Yilun Wang, and Hang Zhao. Hdmapnet: An online hd map construction and evaluation framework. In *ICRA*, 2021. 2, 4, 5, 6
- [16] Tianhong Li, Huiwen Chang, Shlok Kumar Mishra, Han Zhang, Dina Katabi, and Dilip Krishnan. Mage: Masked generative encoder to unify representation learning and image synthesis. In *CVPR*, 2023. 3
- [17] Tianyu Li, Li Chen, Huijie Wang, Yang Li, Jiazhi Yang, Xiangwei Geng, Shengyin Jiang, Yuting Wang, Hang Xu, Chunjing Xu, Junchi Yan, Ping Luo, and Hongyang Li. Graph-based topology reasoning for driving scenes. *arXiv preprint arXiv:2304.05277*, 2023. 3, 6
- [18] Zhiqi Li, Wenhai Wang, Hongyang Li, Enze Xie, Chonghao Sima, Tong Lu, Yu Qiao, and Jifeng Dai. Bevformer: Learning bird’s-eye-view representation from multi-camera images via spatiotemporal transformers. In *ECCV*, 2022. 2
- [19] Bencheng Liao, Shaoyu Chen, Xinggong Wang, Tianheng Cheng, Qian Zhang, Wenyu Liu, and Chang Huang. Maptr: Structured modeling and learning for online vectorized hd map construction. In *ICLR*, 2022. 3, 5, 6
- [20] Bencheng Liao, Shaoyu Chen, Yunchi Zhang, Bo Jiang, Qian Zhang, Wenyu Liu, Chang Huang, and Xinggong Wang. Maptrv2: An end-to-end framework for online vectorized hd map construction. *arXiv preprint arXiv:2308.05736*, 2023. 3, 4, 6
- [21] Jihao Liu, Xin Huang, Jinliang Zheng, Yu Liu, and Hongsheng Li. Mixmae: Mixed and masked autoencoder for efficient pretraining of hierarchical vision transformers. In *CVPR*, 2023. 3
- [22] Xiaolu Liu, Song Wang, Wentong Li, Ruizi Yang, Junbo Chen, and Jianke Zhu. Mgmmap: Mask-guided learning for online vectorized hd map construction. In *CVPR*, 2024. 6
- [23] Yinhan Liu, Myle Ott, Naman Goyal, Jingfei Du, Mandar Joshi, Danqi Chen, Omer Levy, Mike Lewis, Luke Zettlemoyer, and Veselin Stoyanov. Roberta: A robustly optimized bert pretraining approach. *arXiv preprint arXiv:1907.11692*, 2019. 3
- [24] Yingfei Liu, Tiancai Wang, X. Zhang, and Jian Sun. Petr: Position embedding transformation for multi-view 3d object detection. *ECCV*, 2022. 3
- [25] Yicheng Liu, Yue Wang, Yilun Wang, and Hang Zhao. Vectormapnet: End-to-end vectorized hd map learning. In *ICML*, 2022. 2, 5
- [26] Zihao Liu, Xiaoyu Zhang, Guangwei Liu, Ji Zhao, and Ningyi Xu. Leveraging enhanced queries of point sets for vectorized map construction. In *ECCV*, 2024. 6
- [27] Limeng Qiao, Wenjie Ding, Xi Qiu, and Chi Zhang. End-to-end vectorized hd-map construction with piecewise bézier curve. In *CVPR*, 2023. 2

- [28] Evan Shelhamer, Jonathan Long, and Trevor Darrell. Fully convolutional networks for semantic segmentation. In *CVPR*, 2015. 3
- [29] R’emy Sun, Li Yang, Diane Lingrand, and Fr’ed’eric Precioso. Mind the map! accounting for existing map information when estimating online hdm maps from sensor data. *arXiv preprint arXiv:2311.10517*, 2023. 2, 3, 6
- [30] Matthew Tancik, Pratul P. Srinivasan, Ben Mildenhall, Sara Fridovich-Keil, Nithin Raghavan, Utkarsh Singhal, Ravi Ramamoorthi, Jonathan T. Barron, and Ren Ng. Fourier features let networks learn high frequency functions in low dimensional domains. In *NeurIPS*, 2020. 4
- [31] Huijie Wang, Tianyu Li, Yang Li, Li Chen, Chonghao Sima, Zhenbo Liu, Bangjun Wang, Peijin Jia, Yuting Wang, Shengyin Jiang, Feng Wen, Hang Xu, Ping Luo, Junchi Yan, Wei Zhang, and Hongyang Li. Openlane-v2: A topology reasoning benchmark for unified 3d hd mapping. In *NeurIPS*, 2023. 3, 5
- [32] Shuo Wang, Fan Jia, Yingfei Liu, Yucheng Zhao, Zehui Chen, Tiancai Wang, Chi Zhang, Xiangyu Zhang, and Feng Zhao. Stream query denoising for vectorized hd map construction. *ECCV*, 2024. 6
- [33] Benjamin Wilson, William Qi, Tanmay Agarwal, John Lambert, Jagjeet Singh, Siddhesh Khandelwal, Bowen Pan, Ratnesh Kumar, Andrew Hartnett, Jhony Kaesemodel Pontes, Deva Ramanan, Peter Carr, and James Hays. Argoverse 2: Next generation datasets for self-driving perception and forecasting. In *NeurIPS*, 2021. 5
- [34] Dongming Wu, Jiahao Chang, Fan Jia, Yingfei Liu, Tiancai Wang, and Jianbing Shen. Topomlp: An simple yet strong pipeline for driving topology reasoning. *ICLR*, 2024. 3
- [35] X. Xiong, Yicheng Liu, Tianyuan Yuan, Yue Wang, Yilun Wang, and Hang Zhao. Neural map prior for autonomous driving. In *CVPR*, 2023. 2, 3, 5
- [36] Zhenhua Xu, Kenneth K. Y. Wong, and Hengshuang Zhao. Insmapper: Exploring inner-instance information for vectorized hd mapping. In *ECCV*, 2024. 3
- [37] Tianyuan Yuan, Yicheng Liu, Yue Wang, Yilun Wang, and Hang Zhao. Streammapnet: Streaming mapping network for vectorized online hd map construction. In *WACV*, 2024. 6
- [38] Gongjie Zhang, Jiahao Lin, Shuang Wu, Zhipeng Luo, Yang Xue, Shijian Lu, Zuoguan Wang, et al. Online map vectorization for autonomous driving: A rasterization perspective. In *NeurIPS*, 2024. 2
- [39] Xiaoyu Zhang, Guangwei Liu, Zihao Liu, Ningyi Xu, Yunhui Liu, and Ji Zhao. Enhancing vectorized map perception with historical rasterized maps. In *ECCV*, 2024. 3
- [40] Zhixin Zhang, Yiyuan Zhang, Xiaohan Ding, Fusheng Jin, and Xiangyu Yue. Online vectorized hd map construction using geometry. In *ECCV*, 2024.
- [41] Yi Zhou, Hui Zhang, Jiaqian Yu, Yifan Yang, Sangil Jung, Seung-In Park, and ByungIn Yoo. Himap: Hybrid representation learning for end-to-end vectorized hd map construction. In *CVPR*, 2024. 3